Sciences & Technologie A – N°39, Juin 2014, 107-117

Synthesis and characterization of the hybrid Ni-TiO_2/PANI for an efficient hydrogen photoproduction under visible light

Mohamed FaouziNsib[a,b*], Samira Saafi[a], Ali Rayes[a,b], AmmarHouas[a,c]

[a]URCMEP (UR11ES85), Faculty of Sciences, University of Gabès, 6029 Gabès,Tunisia
[b] National School of Engineers (ENIG), University of Gabès, 6029 Gabès,Tunisia
[c]Al Imam Mohammad Ibn Saud Islamic University (IMSIU), College of Sciences, Department of Chemistry, Riyadh 11623, Saudi Arabia

Reçu le 12/05/2014 – Accepté le 24/06/2014

Abstract

$Ni_xZn_{1-x}O$/Polyaniline hybrid photocatalysts are synthesized by the impregnation method at ambient temperature and used for hydrogen photoproduction experiments. XRD, UV-Vis DRS, SEM and TGA are used to characterize the prepared materials. It is shown that the Ni^{2+} amount doped into ZnO controls its morphology and enhances its photoactivity for H_2 generation. Polyaniline (PANI) is shown to sensitize ZnO and to extend its light absorption toward the visible region. The hybrid photocatalyst with 10 mol. % Ni^{2+} and 10 wt. % PANI shows the maximum photocatalytic H_2 production for one hour of visible irradiation: ~ 558 µmole while only ~ 178 µmole in the presence of pure ZnO. It is also observed that the hydrogen photoproduction efficiency depends strongly on the nature of the sacrificial electron donor and increases in the order: thiosulfate >sulfide> propanol.

Key words:photocatalysis; Ni dopedZnO; polyaniline; hydrogen production.

Résumé

Des photocatalyseurshybrides $Ni_xZn_{1-x}O$/Polyanilinesont synthétisés parla méthoded'imprégnationà température ambiante etutiliséspour des expériences dephotoproductiond'hydrogène.DRX,UV-VisSRD, MEBetATGsont utilisées pour caractériserlesmatériaux préparés. Il est montré quelaquantitéde Ni^{2+}dopée en ZnOcontrôlesamorphologieetamélioresaphotoactivitépour la production d'H_2. Polyaniline(PANI) permet de sensibiliserZnOet d'étendre sonabsorption de la lumièreversla zone visible. Le photocatalyseurhybrideavec10mol. (%) enNi^{2+}et10mass. (%) enPANIpermet la productionphotocatalytique maximale deH_2pendant une heured'irradiationvisible: ~558µmol, tandis que seulement ~178µmolen présence deZnOpur. Il est également observé que l'efficacitédelaphotoproductiond'hydrogènedépend fortement de lanature du donneursacrificiel d'électronsetaugmente dans l'ordre: thiosulfate>sulfure>propanol.

Mots clés : photocatalyse, Ni-ZnO, polyaniline, production d'hydrogène, dissociation de l'eau.

ملخص

وقع تحضيرالمحفزات الضوئية الهجينة من نوع بواسطة طريقة التشريب في درجة حرارة عادية و ذلك لاستخدامها في تجاربالإنتاج الضوئي للهيدروجين. تقنيات

XRD و SEM و UV-Vis DRS و TGA

وقع استعمالها لتوصيف المواد المعدة. و تبين أن كمية كاتيونات النيكل المزروعة في أكسيد الزنك لها تأثير على تشكل الأكسيد و تحسن فاعليته في الانتاج الضوئي للهيدروجين. البولي أنيلين ساعد على تحسين حساسية أكسيد الزنك للضوءوتمديد منطقة امتصاصه للضوءتجاهالمنطقة المرئية.
المحفز الضوئي الهجين المحتوي على 10 ٪ مول نيكل و 10٪ وزن بولي أنيلين مكن من انتاج أقصى للهيدروجين لمدة ساعة واحدة من التعرض للأشعة المرئية : ~ 558 ميكرومول مقابل ~ 178 فقط في وجودأكسيدالزنكالنقي.لوحظأيضاأنكفاءةإنتاجالهيدروجين بفعل التحفيز الضوئيتعتمدبقوةعلىطبيعةالجهة المضحية المانحة للإلكترونات، و هذه الكفاءة تزداد حسب النظام التالي: ثيوسلفات>كبريتيد>بروبانول.

الكلمات المفتاحيةتحفيز ضوئي، نيكل-أكسيد الزنك، بولي أنيلين، انتاج الهيدروجين، تقسيم الماء

1. Introduction

Hydrogen is considered the future fuel that may solve the global energy and environmental problems. It is clean and energy efficient **[1, 2]**. Produced without carbon dioxide or any other greenhouse gas affecting the climate, hydrogen can form the basis of a truly sustainable energy **[3, 4]**. At present, several hydrogen-producing technologies exist, such as those based on fossil fuels, natural gas reforming, bio-derived liquids reforming, coal and biomass gasification, thermochemical and nuclear production, or water electrolysis [**5-9]**. However, these technologies are either expensive or environmentally unfriendly.

Heterogeneous photocatalysis is a low cost and environmentally-friendly procedure that has been well-studied for the wastewater/air treatment **[10-13].** In recent years, photocatalytic water splitting into hydrogen has attracted many researchers. But, when developing photocatalysts, it is particularly important to find a material with a lower energy band gap (Eg) that enables the efficient use of solar energy to produce hydrogen **[14-17]**.

Zinc oxide (ZnO) has been considered a promising semiconductor to support the future hydrogen economy because it has distinctive optoelectronic, catalytic, and photochemical properties**[18]**. The quantum efficiency of ZnO is also significantly larger than titanium dioxide (TiO_2)**[19, 20]**. However, the energy conversion efficiency from solar to hydrogen by photocatalytic water splitting is still low, due to these main reasons: (i) Recombination of photogenerated electron/hole pairs, (ii) Fast backward recombination of hydrogen and oxygen into water, and (iii) Inability to use the visible part of the sunlight.

To resolve the above problems and make solar photocatalytic hydrogen production feasible, first we need to use chemical additives (electron donors, noble metals, carbonate salts,…) to avoid the electron/hole and O_2/H_2recombinations**[21].** Second, it is needed to modify the photocatalyst to make it active under visible light **[22, 23]**. Particularly, it is reported that modifying ZnO with transition metal ions such as Ni^{2+} can inhibit charge recombination **[24]**. Besides, the Ni^{2+} ions can increase the surface defects and presumably shift the light absorption towards the visible region **[25]**. This may be reached by the p-n junction concept. In this concept, the hetero-junction of a p-type material such as NiO with its n-type counterpart (ZnO) induces an internal electric field which may extend the probability of electron-hole separation **[26]**.

On the other hand, it is reported that the associationofZnOwith a functional polymerinahybrid material isexpectedtoimproveits morphology. In addition,organicmoleculesallow a better coverageofthe solar emission spectrum, especially when the organic and inorganic networksareinterpenetrated**[27-29]**. The hybrid entityis anticipated to benefit from thesynergisticeffectsofphysical and chemicalinteractions which occur between the organic and inorganiccomponents and, so, it may be usedas a photocatalystforefficientH_2productionunder visible andsolar lights **[30-32]**.Polyaniline(PANI) is amongthe most convenientconductive polymers**[33]**. It has extended π-conjugated electron systems and is an efficient electron donor and a good hole transporter upon visible-light excitation **[34]**. PANI has environmental,electrical, opticaland electrochemicalpropertiesandcanbechemicallyandelectrochemically-synthesized **[35-38]**.Furthermore, it has ahighmobilityofcharge carriers andastrongabsorptionin the visiblespectrum due to its low band gap (2.8 eV) **[34]**. Economically, PANI ispreferredbecauseitsmonomer(aniline) is among thecheapest in the market. Consequently, PANI is a well-synthesizing candidate for the organic-inorganic hybrid photocatalyst to produce H_2 from water splitting under visible/solar lights **[39]**.

The aim of this study is to prepare an organic-inorganic hybrid photocatalyst of high photocatalytic activity in water-splitting reaction. The hybrid material is based on Ni doped ZnO as the inorganic component and PANI as the organic one. A series of factors influencing the activities of Ni-ZnO/PANIphotocatalysts for H_2 evolution have been investigated. It is found that the well-prepared Ni-ZnO/PANI composite shows a highphotocatalytic efficiency in sustainable hydrogen production from water splitting under the visible light irradiation.

2. Experimental Part

2.1. Synthesis of Ni-ZnO materials

The Ni-doped ZnOis prepared by homogeneous precipitation usingzinc acetate, oxalicacidand nickel chloride as precursors. 4.8 gof zinc acetateand 2.5g of oxalic acidaredissolved in50ml ofdistilled water understirring for2 h atroom temperature. An amount of nickel chloride, which corresponds to Ni to ZnO molar ratio equal to 1, 5 and 10 %, respectively, is then added to the solution. The obtained precipitate isfiltered, washed withmethanol, dried inan oven at 80°Cfor 24h, and then heated at400 °Cfor 3 h to get a Ni doped zinc oxide (Ni-ZnO).

Pure ZnO is prepared using the same method, but without adding the nickel chloride precursor.

2.2. Synthesis of polyaniline (PANI)

Themethodusedin our preparation of PANIis the oxidative polymerization ofanilinemonomerbyammoniumpersulfate (APS)in aqueous solution of H_2SO_4ata pH of 1to 3. In a typical synthesis, 50 mL of H_2SO_4 solution containing 1.4 g of APS was added drop by drop to 50 mL of H_2SO_4 solution containing 1.82 mL of aniline. The polymerization was allowed to proceed by stirring the mixture for 2 h at ambient temperature. The obtained dark green precipitate corresponding to PANI was then filtered and washed with a large amount of distilled water followed by methanol. The resulting PANI was finally dried for 24 h at 80 °C.

2.3. Synthesis of Ni-ZnO/PANI composites

The Ni-ZnO/PANI composites were prepared by the direct impregnation method. In a typical procedure, 1 g of Ni-ZnO nanoparticles was dispersed in 30 mL of aqueous PANI solution during one hour under stirring. The concentration of the PANI aqueous solution was such as the wt% of PANI in the final Ni-ZnO/PANI hybrid was 3, 6 and 10 %, respectively. The obtained Ni-ZnO/PANI composite powders were filtered, washed three times with ethanol and water respectively, and dried for 24 h at 80 °C. The Ni-ZnO/PANI composites were labeled Ni_x-$Zn_{1-x}O$/$PANI_y$ where x (x = 1, 5 and 10 %) and y (y = 3, 6 and 10) are the Ni to ZnO molar ratio and the wt.% of PANI in the Ni-ZnO/PANI composite, respectively.

2.4. Characterization of Ni-ZnO nanoparticles and Ni-ZnO/PANI hybrids

The Ni-ZnO nanoparticles and Ni-ZnO/PANI hybrids were characterized by XRD, SEM, TGA and DRS UV-Vis.

The X-ray diffraction (XRD) patterns obtained on a SIEMENS HT/BT X-ray diffractometer using Cu Kα radiation at a scan rate of $0.02^\circ\ s^{-1}$ were used to decide the identity of ZnO and the crystallite size of the powders. The average crystallite size was determined according to Scherrer's equation: $d = k.\lambda / \beta.\cos\Theta$, where k is the shape factor of particles equal to 0.89, β is the peak width at half maximum (in radians), λ is the X-ray wavelength (0.15418 nm), and Θ is the Bragg angle.

The Scanning electron micrograph (SEM) was recorded with a Neoscope JCM-5000 (JEOL Company, Japan) electron microscope and was used for observing the shape and morphology of the prepared particles.

A UV-Vis 3101 PC (UV Probe Shimadzu) was used to record the diffuse spectra (DRS) of the samples. Reflectance spectra were analyzed under ambient condition in the wavelength range of 200-800 nm.

TGA experiments of the prepared pure ZnO and Ni-ZnO/PANIcomposite were performed with aSETERAMthermobalance, in the temperature range of 20–500°C, under a dynamic atmosphere of argon. Samples were put into platinum crucibles, at a heating rate of 10 °C min^{-1}.

2.5. Photocatalytic hydrogen production experiments

The typical liquid-phase photocatalytic reactor **[40, 41]** used in our laboratory for H_2 production is shown in the Fig.1. This photocatalytic reactor of 100 mL was irradiated with an outer 250 W halogen visible lamp. In each experiment, 1 $g.L^{-1}$ of a photocatalyst and 0.2 M of $Na_2S_2O_3$ as a sacrificial electron donor were used. Sodium carbonate salt (Na_2CO_3) was used as electron mediator to prevent the fast backward reaction of hydrogen and oxygen **[21]**. Before illumination, the aqueous slurry was deaerated with N_2 gas and kept in the dark for 30 min. During irradiation, the evolved H_2 gas was collected and volumetrically-measured in a water displacement graduated burette. All experiments were carried out under the same conditions and blank test was performed to determine the H_2 photolysis volume. However, in the absence of light, the dark control showed no noticeable H_2 production.

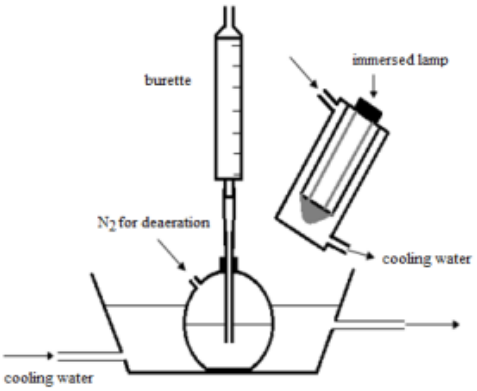

Fig.1. Schematic diagram showing liquid-phase photocatalytic H_2 production from water-splitting.

3. Results and discussion

3.1 Materials characterization

3.1.1X ray diffraction

The Fig. 2 shows the XRD patterns of the fine powdersof prepared pureZnO and $Ni_{0.1}Zn_{0.9}O$. They showpeaksatpositions 2θ =31.63°, 34.22°, 36.03°, 47.3°, 56.43°, 62.79°, 66.31°, 67.84°and69.05°, whichcorrespond to thereflectionplanes(100), (002), (101), (102), (110) (103), (200), (112) and(201), respectively. They are

in good agreement with the standard JCPDS file (36-1451)for the hexagonal wurtzite structure of ZnO. Moreover, no change in the wurtzite structure of ZnO after Ni doping is observed, which indicates that Ni^{2+} occupies the Zn^{2+} site into the crystal lattice **[42]**. An additional peak corresponding to NiO is shown at 2θ= 43.20° in the $Ni_{0.1}Zn_{0.9}O$ pattern. This new peak clearly indicates that a segregation phase occurred in the $Ni_{0.1}Zn_{0.9}O$ sample. So, a p-n heterojunction may take place between NiO and ZnO oxides in the Ni doped ZnO sample, which is expected to enhance the electron/hole separation.

On the whole, the diffraction peaks are sharp, narrow and symmetrical with a low and stable baseline, suggesting that the samples are well-crystallized **[43].**

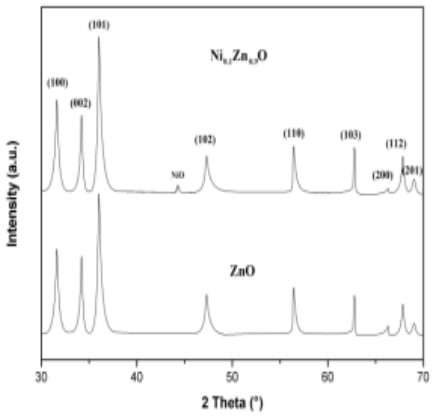

Fig.2. XRD profiles of prepared pure ZnO and $Ni_{0.1}Zn_{0.9}O$.

The average values of the crystalline size of the samples are calculated using the Debye-Scherrer equation and the half width of the (101) crystal plane. It is found that the ZnO crystalline size varies weakly with the Ni doping and takes the average values of 22.6 and 25.7 nm for ZnO and $Ni_{0.1}Zn_{0.9}O$, respectively. This is probably due to the slight difference between the ionic radius of Zn^{2+} (0.74 Å) and Ni^{2+} (0.69 Å).

3.1.2 Scanning Electron Microscopy (SEM)

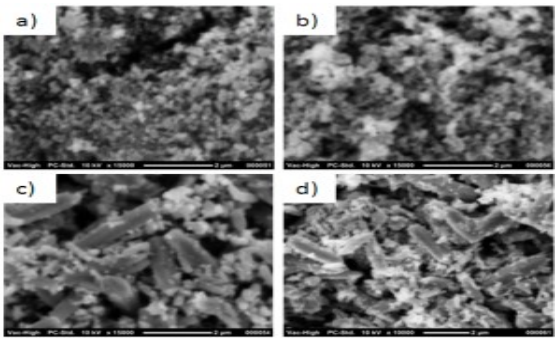

Fig.3. SEM images of bare ZnO nanoparticles (a), $Ni_{0.01}Zn_{0.99}O$ (b), $Ni_{0.05}Zn_{0.95}O$ (c) and $Ni_{0.05}Zn_{0.95}O/PANI_3$ (d) photocatalysts.

The influence of different molar ratios of Ni^{2+} on the surface morphologies of the photocatalysts was studied by SEM (Fig.3). The SEM images of pure ZnO (a) and 1 % Ni-doped ZnO (b) show low aggregation of particles which have spherical morphology and are evenly distributed on the whole surface. However, the increase of the Ni content to 5 mol. % changes drastically the morphology of the Ni-ZnO particles (c). Thus, the $Ni_{0.05}Zn_{0.95}O$ particles are more aggregated and have nanorods-like morphology. The nanorods are quite uniform in size. Similar morphology is observed in the $Ni_{0.1}Zn_{0.9}O$ sample (not shown here). These observations show that Ni content controls the growth of Ni doped ZnO crystals. Ni^{2+} anions may act as a catalyst to promote the one dimensional growth of ZnOnanocrystals. In this case, Ni^{2+} may act as a nucleation site and help the growth of arrays of ZnO when the Ni^{2+} content reaches 5 mol. %.The nanorods-like morphology is maintained when $Ni_{0.05}Zn_{0.95}O$ is hybridized with PANI (d). The nanorod morphology is expected to enhance the photosensitivity as well as the photoresponse**[44]**.

3.1.3 UV-Vis diffuse reflectancespectra (DRS)

UV–Vis diffuse reflectance spectroscopy, which is generally used to detect the presence of framework and non-framework incorporated transition metal species in the structures and to distinguish the coordination states of the metal ions **[45, 46]**, was used here to provide some insights into the interactions of the photocatalyst materials with photon energies.

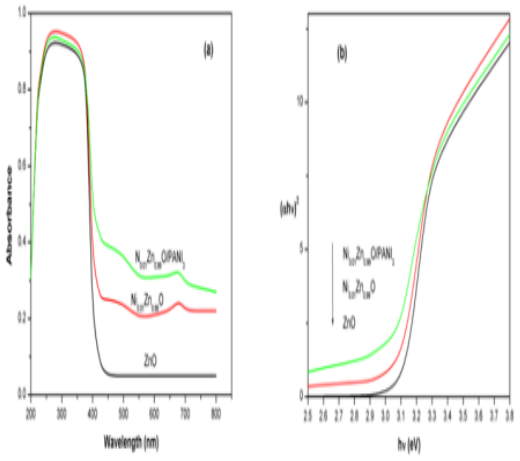

Fig. 4.UV–Vis spectra of ZnO, $Ni_{0.01}Zn_{0.99}O$ and $Ni_{0.01}Zn_{0.99}O/PANI_3$nanocomposite (a) and the corresponding plot of $(\alpha h\nu)^2$ vs. hν (b).

Fig.4a illustrates the UV-Vis diffuse reflectance full spectra of bare ZnO, $Ni_{0.01}Zn_{0.99}O$ and $Ni_{0.01}Zn_{0.99}O/PANI_3$photocatalysts. It is obvious that the bare ZnO absorbs light with wavelengths only below 390 nm. The spectrum of ZnO consists of a single absorption usually ascribed to charge-transfer from the valence band (formed by 2p orbitals of the oxide anions) to the conduction band (formed by 3d orbitals of the Zn^{2+}cations). It is clear from Fig.4a that the absorbance of Ni-doped ZnO nanoparticles in the visible region is higher than that of pure ZnO nanoparticles.It is assumed that the enhanced optical activity is owed to the increase in the surface imperfections due to Ni doping in ZnO nanoparticles, which is expected to be driven by the interaction of the Ni 3d and O 2p states in both the valence and conduction bands **[47]**.It means that defect sites are generated in the vicinity of valence band due to doping of ZnO with Ni ions. As a result, electron-hole pair is generated within the effective band gap after photoexcitation of particles, and electron transition takes place from the defect valence state to the defect conduction state. This transition requires much lower energy than the band gap of ZnO.

After being sensitized by PANI, the $Ni_{0.01}Zn_{0.99}O/PANI_3$ composite photocatalyst can not absorb only the UV light, but can also considerably absorb visible light. We observed a noticeable shift of the optical absorption edge for the Ni-ZnO/PANI system towards the visible region. Surely, this shift towards the longer wavelengths originates from the band gap narrowing of Ni-ZnO by PANI hybridization.
The band gap as calculated for pure ZnO,$Ni_{0.01}Zn_{0.99}O$ and$Ni_{0.01}Zn_{0.99}O/PANI_3$ is 3.12, 3.07 and 2.98 eV, respectively.
The band gap energy of the photocatalysts samples was determined using the Tauc equation **[48]**:
$\alpha h\nu = A\,(h\nu - E_g)^n$
Where α is the absorption coefficient, A is a constant and n = ½ for direct band gap semiconductor. An extrapolation of the plot of $(\alpha h\nu)^2$ vs. $h\nu$ (Fig.4b) gives the value of the band gap **[49, 50]**.

The above results indicate that PANI is able to sensitize ZnO efficiently. The resulting composite photocatalysts can be excited by absorbing both UV and visible light to produce more electron-hole pairs and give a maximum visible-light harvesting. This, in turn, can result in higher photocatalytic activities, and therefore, it can be a promising photocatalytic material for the efficient use of light, especially sunlight in the photoproduction of hydrogen.

3.1.3 Thermal analysis

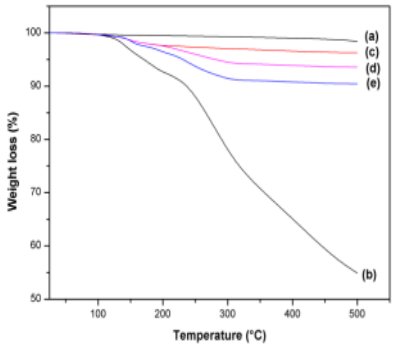

Fig.5. TGA curves of $Ni_{0.01}Zn_{0.99}O$ (a), PANI (b), $Ni_{0.01}Zn_{0.99}O/PANI_3$ (c), $Ni_{0.01}Zn_{0.99}O/PANI_6$ (d) and $Ni_{0.01}Zn_{0.99}O/PANI_{10}$ (e).

The thermal behavior of the hybrid photocatalysts was investigated by thermogravimetry (TG) in comparison to prepared $Ni_{0.01}Zn_{0.99}O$ and PANI samples. The results are illustrated in Fig.5.As it is clearly seen, the prepared $Ni_{0.01}Zn_{0.99}O$ proves a good thermal stability till 500 °C; only 1.36 % of weight loss, which is probably attributed to absorbed moisture, is shown. The TG curve of prepared pure PANI shows first weight loss of 7.3 % due to absorbed moisture and solvent upon initial heating up to 200 °C. A secondweight loss occurs from 220 to 500 °C and corresponds to the degradation phase of the polymer. The final degradation of PANI should be occurred around 600-750 °C **[51]**. On the other hand, the weight loss shown in the thermograms of Ni-ZnO/PANI nanocomposites may be due to the decomposition of the organic moiety. Obviously, this weight loss mainly occurring from 200 to 500 °C increases with the proportion of PANI in the hybrid material. Moreover, the weight losses are smaller than the nominal amounts of PANI in the nanocomposites (Table.1).Two reasons may explain this result: i) the given weight losses are those calculated at 500 °C, before the total degradation of PANI and ii) it is not certain that all the initial amount of PANI was effectively used to impregnate the inorganic moiety of the hybrid nanocomposite.

Table.1.wt.% of PANI from TGA curves in comparison to nominal values in the Ni-ZnO/PANI hybrids.

Nominal wt.% of PANI	wt.% of PANI from TGA
3	2.13
6	4.85
10	7.95

3.2. Photocatalytic hydrogen production in the presence of $Ni_xZn_{1-x}O/PANI_y$

3.2.1 Effect of Ni^{2+} content

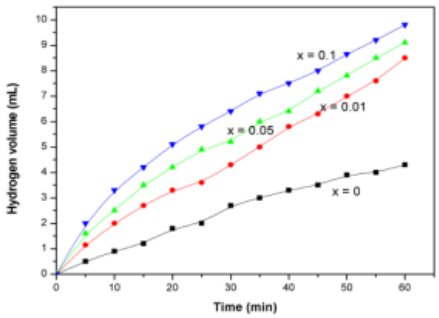

Fig.6. Effect of Ni^{2+} content on the volume of H_2evolution ($V_{solution}$ = 100 mL, catalyst = 0.1 g$Ni_xZn_{1-x}O/PANI_3$; x = 0, 0.01, 0.05 and 0.1, electron donor: $Na_2S_2O_3$).

The effect of Ni^{2+} content on the photocatalytic activity of the Ni-ZnO/PANI material under visible light is examined while keeping constant the amount of PANI in the hybrid composition. Fig.6 presents the time course of the photocatalytic hydrogen generation by $Ni_xZn_{1-x}O/PANI_3$ photocatalyst with different Ni^{2+} content. It is clearly shown that doping ZnO with Ni^{2+}cations significantly increase its activity for the hydrogen photoproduction under visible illumination. For one hour of visible irradiation, the hydrogen production of $Ni_xZn_{1-x}O/PANI_3$photocatalysts reached the points of 8.5 mL (~ 379 µmole), 9.1 mL (~ 406 µmole) and 9.8 mL (~ 437 µmole) for x = 0.01, 0.05 and 0.1, respectively. These productions are much higher than of pure ZnO on the same reaction condition, which is only 4 mL (~ 178 µmole). The large difference between the efficiency of Ni-doped and undopedZnO can be explained by two main factors: The ability to absorb visible light and to separate the photogenerated charges.

As shown above by DRS results, Ni doped ZnO absorbs more visible light and so act as a better photocatalyst under visible light irradiation. Besides enhancing the ability to absorb visible light, Ni doping is expected to enhance the separation of electron and hole and avoid their fast recombination owing to the p-n junction concept. It means that the contact between NiO, as a p-type semiconductor, with ZnO, as a n-type counterpart, is expected to induce an internal electric field that can extend the probability of electron-hole separation **[52]**.

3.2.2. Effect of PANI amount

The effect of the PANI amount on the hydrogen production is investigated using $Ni_{0.1}Zn_{0.9}O/PANI_y$photocatalysts. Fig.7 describes the obtained results when y values are respectively 3, 6 and 10 wt.%. It is found that the hybridization of Ni-ZnO with PANI improves its photocatalytic activity under visible light irradiation. As a result, the volume of hydrogen photoproduced increased in the presence of $Ni_{0.1}Zn_{0.9}O/PANI_y$photocatalysts compared to the non hybridized $Ni_{0.1}Zn_{0.9}O$. This enhancement is found to be more pronounced when the amount of PANI in the $Ni_{0.1}Zn_{0.9}O/PANI_y$composite increase. Thus, for one hour of visible irradiation, the volume of photoproduced hydrogen reaches 9.8 mL (~ 437 µmole) with $Ni_{0.1}Zn_{0.9}O/PANI_3$, 10.9 mL (~ 486 µmole) with $Ni_{0.1}Zn_{0.9}O/PANI_6$, 12.5 mL (~ 558 µmole) with $Ni_{0.1}Zn_{0.9}O/PANI_{10}$ and only 6.6 mL (~ 294 µmole) with $Ni_{0.1}Zn_{0.9}O$. The amounts of hydrogen production measured in this work in the presence of Ni-ZnO/PANIhybridphotocatalysts are significantly higher than those found when using some other photocatalysts**[53-55]**. Two reasons may explain why the photocatalytic activity of Ni-ZnO/PANI hybrids is higher than that of pure ZnO or Ni-doped ZnO: (i) Chemical interactions are expected to occur between ZnO nanoparticles and PANI conducting polymer. Consequently, electrons transfer from PANI to ZnO, leading to an increase of electrons density in ZnO. As a result, the amount of photoexcited electrons is increased and the photocatalytic activity of the composites for hydrogen production is improved. (ii) The disordered structure of PANI may be improved and have some ordering after addition of ZnO nanoparticles, which may lead to transferring of electrons from PANI to ZnO becoming easier. Subsequently, electrons are easily photoexcited in ZnO and the photocatalytic activity of Ni-ZnO/PANI composites for hydrogen evolution is improved.

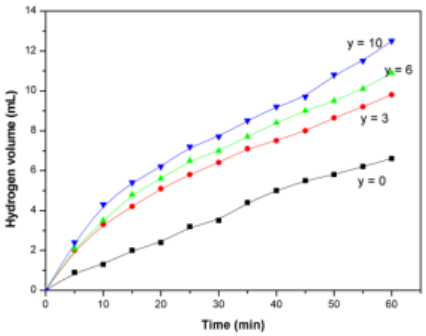

Fig.7. Effect of PANI wt.% on the volume of hydrogen evolution ($V_{solution}$ = 100 mL, catalyst = 0.1 g$Ni_{0.1}Zn_{0.9}O$/$PANI_y$, y = 3, 6 and 10, electron donor: $Na_2S_2O_3$).

In other words, it is suggested that the hybridization of ZnO with the conducting polymer leads to the increase of the rate of electron transfer to the ZnO surface. This behavior plays a considerable role of increasing hydrogen production. In fact, as the surface of ZnO is saturated by the accumulated photoexcited electrons, the Fermi level shifts nearer to the conduction band, and the energy moves into the more negative level. Besides, the accumulated electrons will be transferred into the protons which are adsorbed at the catalyst surface. Hence, the protons are reducedintohydrogen.

3.2.3 Effect of the nature of the sacrificial electron donor

Fig.8 shows the photocatalytic hydrogen evolution activities over a $Ni_{0.1}Zn_{0.9}O$/$PANI_{10}$ photocatalyst from various sacrificial electron donor solutions. Here, sulfide (S^{2-}), thiosulfate ($S_2O_3^{2-}$) and propanol (C_3H_7OH) are used as electron donor, respectively. The reactions were conducted with electron donor concentrations of 0.2 $mol.L^{-1}$. It should be noticed that in all experiments, any noticeable hydrogen volume is measured in the absence of electron donor, which reject the possibility of distilled water-splitting. Besides, it is shown that the hydrogen evolution over $Ni_{0.1}Zn_{0.9}O$/$PANI_{10}$ photocatalyst is quite stable in the presence of the tested sacrificial electron donors. This finding shows that these electron donors react irreversibly with the photoinduced holes. Moreover, it is observed that the hydrogen photoproduction efficiency depends strongly on the nature of the sacrificial electron donor and increases in the order: thiosulfate >sulfide> propanol. For one hour of visible irradiation, the volumes of photoproduced hydrogen are: 12.5 mL ~ 558 µmole (thiosulfate), 9.3 mL ~ 415 µmole (sulfide), and 7.7 mL ~ 343 µmole (propanol).

The photocatalytic hydrogen generation in the presence of propanol may take place stepwise involving intermediates such as aldehydes and acids, which may compete between them and propanol with the valence band holes (h^+) **[56]**. This may partially explain the decrease of the amount of hydrogen photoproduced in the presence of propanol compared to S^{2-} and $S_2O_3^{2-}$. Under our experimental conditions (pH = 7-8), sulfide ions (S^{2-}) are less abundant in the electron donor solution than bisulfide ions HS^- (pk_{a2} (HS^-/S^{2-}) = 13). HS^- can trap easily the valence band holes during a single stepwise reaction **[57]**:

$$HS^- + h^+ \longrightarrow HS^{\cdot} \quad \textbf{(1)}$$

The small amount of S^{2-} present in the solution may diffuse slower than HS^- to the photocatalyst surface and react with holes as follows:

$$S^{2-} + h^+ \longrightarrow S^{\cdot-} \quad \textbf{(2)}$$

Thiosulfate anions ($S_2O_3^{2-}$) are the most efficient electron donors experimented here; they potentially increase the reaction rate of the photocatalytic hydrogen generation. The photogenerated semiconductor holes (h^+) are scavenged by the added $S_2O_3^{2-}$ anions. $S_2O_3^{2-}$ anions are oxidized by direct electron transfer to the photogenerated holes during a single stepwise reaction:

$$2\ S_2O_3^{2-} + 2\ h^+ \longrightarrow S_4O_6^{2-} \quad \textbf{(3)}$$

This should lead to a decrease of the electron/hole recombination and, consequently, the photoinjected electrons in the semiconductor conduction band are increased and rapidly delivered to the pre-adsorbed H^+ to produce H_2:

$$2H^+ + 2\ e^-_{cb} \longrightarrow H_2 \quad \textbf{(4)}$$

Because the standard redox potentials of $HS^-/HS^{\cdot}$ and $S_2O_3^{2-}/S_4O_6^{2-}$ couples are 1.08 and 0.08 V, respectively, thiosulfate oxidation would take place more efficiently than that of sulfide/bisulfide. Thus, photocatalytic hydrogen evolution is more effective in the presence of thiosulfate anions as sacrificial electron donors.

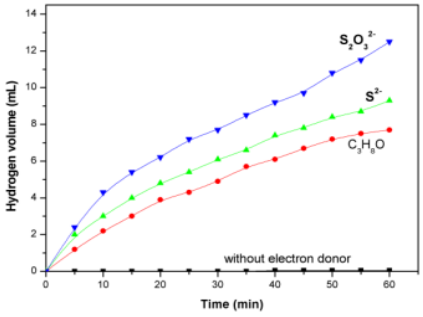

Fig.8. Effect of the nature of the added electron donor on the volume of hydrogen evolution ($V_{solution}$ = 100 mL, catalyst = 0.1 g$Ni_{0.1}Zn_{0.9}O$/$PANI_{10}$).

The above results suggest that the rate of H_2 production is mainly governed by the reduction potential of the sacrificial electron donor and by the kinetic of the electron transfer process. The adsorption behavior of the electron donors is may be another important factor that can explain the difference in hydrogen evolution between the three donors. However, their exact adsorption nature is remained uncertain, so an investigation of the surface reactions is ongoing.

3.2.4 Effect of photocatalyst loading

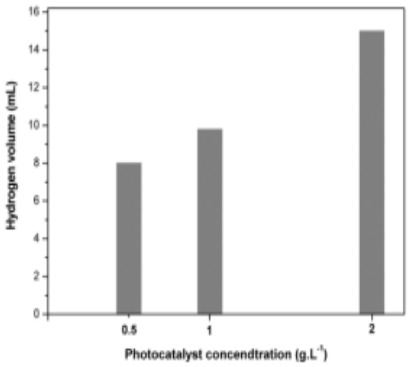

Fig.9. The effect of $Ni_{0.1}Zn_{0.9}O/PANI_3$ content on the amount of evolved H_2 ($V_{solution}$ = 100 mL, electron donor: $Na_2S_2O_3$).

One of the operational parameters which can affect the photocatalytic hydrogen generation is the catalyst loading. This is illustrated in Fig.9 for $Ni_{0.1}Zn_{0.9}O/PANI_3$ photocatalyst amount of 0.5, 1 and 2 $g.L^{-1}$, respectively. $S_2O_3^{2-}$ was used as the electron donor. It is shown that the amount of H_2photogenerated increases with increasing the catalyst loading. For one hour of irradiation, the H_2 volume reaches about 8, 10 and 15 mL in the presence of 0.5, 1 and 2 $g.L^{-1}$ of catalyst concentration, respectively. The above results show that the suspended $Ni_{0.1}Zn_{0.9}O/PANI_3$ did not reduce the penetration of the light in the solution and no severe light scattering was occurred for larger catalyst loading (2 $g.L^{-1}$). It means that the number of available photons inside the photoreactor increased with the amount of the catalyst.

3.2.5 Photocatalytic mechanism of H_2 generation

The increase in the photocatalytic activity of Ni-ZnO/PANI compared to bare ZnO should be essentially attributed to the efficient separation of electron and hole pairs. Both Ni^{2+} ions and PANI have significant contribution and great influence on the photocatalytic activity of Ni-ZnO/PANI composite for the hydrogen production. It can be hypothesized that Ni^{2+} doping into the ZnO lattice introduces an additional electron energy level into the valence band, which may reduce the energy band gap **[58, 59]**. When Ni-ZnO/PANI composite is illuminated under visible light, both Ni-ZnO and PANI absorb the photons at their interface. Since the lowest unoccupied molecular orbital (LUMO) level is more negative than that of the CB of ZnO, then, the electrons photogenerated from PANI can be transferred into the CB of ZnO where protons can be reduced to hydrogen. On the other hand, the photogenerated holes are consumed by reacting with the added carbonate species to form carbonate radicals ($HCO_3^{\cdot}$) and may be CO_2, which can promote the desorption of O_2 from the photocatalyst surface and minimize the formation of H_2O through the backward reaction of H_2 and O_2**[21]**. All these possibilities are shown in the schematic diagram of the schema.1.

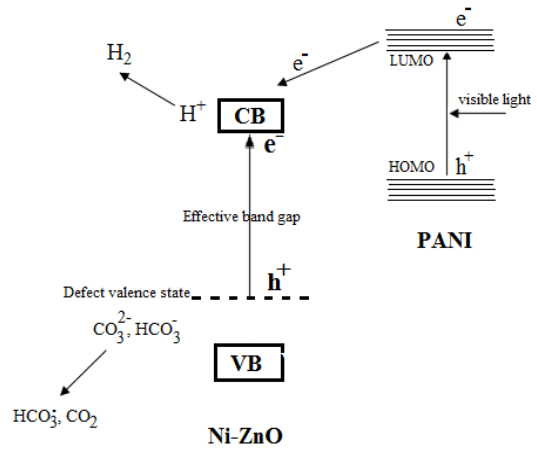

Schema.1. Schematic diagram of possible mechanisms of hydrogen photoproduction in the presence of Ni-ZnO/PANI photocatalyst.

4 Conclusion

Ni-ZnO/PANI hybrid photocatalysts were prepared by a simple impregnation method. As the organic partner, PANI can extend the photoresponse of ZnO to the visible region and narrow its band gap energy. The Ni2+ ions were found to substitute Zn^{2+} into the ZnO lattice and its content was shown to control the ZnO morphology. Through this research, we found that Ni^{2+} ions and PANI both have great influence on the photocatalytic activity of Ni-ZnO/PANI composite. The $Ni_{0.1}Zn_{0.9}/PANI_{10}$ displayed the highest photoactivity for hydrogen production under visible-light irradiation. Moreover, the nature of the added sacrificial electron donor was found to increase the photoproduction efficiency of

hydrogen in the order: thiosulfate >sulfide> propanol.

References

[1]C-H Liao, C-W Huang, JCS Wu. Hydrogen Production from Semiconductor-basedPhotocatalysis via Water Splitting. Catalysts,2, 2012, 490-516.

[2] Thomas CE, James BD, Lomax Jr FD, Kuhn Jr IF. Fuel Options for the fuel cell vehicle: hydrogen, methanol or gasoline?.Int J Hydrogen Energy,25, 2000, 551-67.

[3]VPreethi, SKanmani.Photocatalytic hydrogen production.Mat SciSemiconProc,16 (3), 2013, 561-75.

[4] X Chen, S Shen, L Guo, S S Mao. Semiconductor-based photo catalytic hydrogen generation.ChemRev,110, 2010, 6503-70.

[5] Damien A. Hydrogène par électrolyse de l'eau. Techniques de l'Ingénieur 1992; J6366.

[6]S Turn, C Kinoshita, Z Zhang, D Ishimura, J Zhou. An experimental investigation of hydrogen production from biomass gasification.Int J Hydrogen Energy, 23(8), 1998, 641-8.

[7] Y Chen, Y Wang, H Xu, G Xiong. Efficient production of hydrogen from natural gas steam reforming in palladium membrane reactor. App Catal B: Environ, 80, 2008, 283-94.

[8] GF Naterer. Hydrogen Production from Nuclear Energy, Chapter 2: Nuclear Energy and Its Role in Hydrogen Production. London:Springer-Verlag, 2013.

[9] C Gaudillere L Naverrete, J M Serra. Syngas production at intermediate temperature through H_2O and CO_2 electrolysis with a Cu-based solid oxide electrolyzercell.Int J Hydrogen Energy, 39, 2014, 3047-54.

[10] F Han, V S R Kambala, M Srinivasan, D Rajarathnam, R Naidu. Tailored titanium dioxide photocatalysts for the degradation of organic dyes in wastewater treatment: A review. ApplCatal A-General, 359(1-2), 2009, 25-40.

[11] MN Chong, B Jin, CWK Chow, C Saint. Recent developments in photocatalytic water treatment technology: A review. Water Res, 44, 2010, 2997-3027.

[12] AA Tellez, R Masson, D Robert, N Keller, V Keller. Comparison of Hombikat UV100 and P25 TiO_2 performance in gas-phase photocatalytic oxidation reactions.JPhotochemPhotobiol A-Chem, 250, 2012, 58-65.

[13] MF Nsib, AMayoufi, N Moussa, N Tarhouni, A Massouri, A Houas, Y Chevalier.TiO_2 modified by salicylic acid as a photocatalyst for the degradation of monochlorobenzene via Pickering emulsion way. J PhotochemPhotobiol A-Chem, 251, 2013, 10-17.

[14] A Kudo. Photocatalysis and solar hydrogen production. Pure Appl. Chem,79 (11), 2007, 1917-27.

[15] A Kudo.Recent progress in the development of visible light-driven powdered photocatalysts for water splitting.IntJHydrogen Energy, 32(14) 2007, 2673-8.

[16] D Jing, L Guo, L Zhao, X Zhang, H Liu, M Li, S Shen, G Liu, X Hu, X Zhang, K Zhang, L Ma, P Guo. Efficient solar hydrogen production by photocatalytic water splitting: From fundamental study to pilot demonstration. IntJHydrogen Energy, 35(13), 2010, 7087-97.

[17] K Villa, X Domènech, S Malato, M I Maldonado, J Peral. Heterogeneous photocatalytic hydrogen generation in a solar pilot plant.Int J Hydrogen Energy, 38 (29), 2013, 12718-24.

[18] AL Stroyuk, VV Shvalagin, SYaKuchmii. Photochemical synthesis and optical properties of binary and ternary metal–semiconductor composites based on zinc oxide nanoparticles.JPhotochemPhotobiol A-Chem,173(2), 2005, 185-194.

[19] FD Mai, CS Lu, CW Wu, CH Huang, JY Chen, CC Chen. Mechanisms of photocatalytic degradation of Victoria Blue R using nano-TiO_2.Sep PurifTechnol,62, 2008, 423-36.

[20]Y Li, W Xie, X Hu, G Shen, X Zhou, Y Xiang, X Zhao, P Fang. Comparison of Dye Photodegradation and its Coupling with Light-to-Electricity Conversion over TiO_2 and ZnO.Langmuir,26, 2010, 591-7.

[21] M Ni, M KH Leung, DYC Leung, K Sumathy. A review and recent developments in photocatalytic water-splitting using $TiO_2$for hydrogen production.RenewSustEnerg Rev,11(3), 2007, 401-25.

[22]H Park, Y Park, W Kim, W Choi. Surface modification of TiO_2 photocatalyst for

environmental applications.JPhotochemPhotobiol C-Rev, 15,2013, 1-20.

[23] R Qiu, D Zhang, Y Mo, L Song, E Brewer, X Huang, Y Xiong. Photocatalytic activity of polymer-modified ZnO under visible light irradiation. J Haz Mater,156, 2008, 80-5.

[24] Z Yin, N Chen, F Yang, S Song, C Chai, J Zhong. Structural, magnetic properties and photoemission study of Ni-doped ZnO. Solid State Commun,135, 2005, 430-3.

[25] S Kant, A Kumar. ZnO and Ni doped ZnOnanospheres prepared by sol-gel method. Adv Mat Lett,3(4), 2012,350-4.

[26] L Li, KS Hui, KN Hui, HW Park, DH Hwang, S Cho, SK Lee, PK Song, YR Cho, H Lee, YG Son, W Zhou. Synthesis and characterization of NiO-doped p-type AZO films fabricated by sol–gel method. Mater Lett,68, 2012, 283-6.

[27] G Kickelbick. Hybrid Materials.Synthesis, Characterization, and Applications.Weinheim: Wiley-VCH Verlag GmbH & Co. KGaA, 2007.

[28] J Huang, Z Yin, Q Zheng. Applications of ZnO in organic and hybrid solar cells.Energ Environ Sci, 4(10), 2011, 3861-77.

[29] S Kango, S Kalia, A Celli, J Njuguna, Y Habibi, R Kumar. Surface modification of inorganic nanoparticles for development of organic-inorganic nanocomposites - A review.Prog Polymer Sci,38, 2013, 1232-61.

[30] Y Yu, J Ren, M Meng. Photocatalytichydrogenevolution on graphene quantum dots anchored TiO_2 nanotubes-array. Int JHydrogenEnergy,38(28), 2013, 12266-72.

[31] Y Wang, X Guo, L Dong, G Jin, Y Wang, X-Y Guo. Enhanced photocatalytic performance of chemically bonded SiC-graphene composites for visible-light-driven overall water splitting.IntJHydrogen Energy,38(29), 2013, 12733-8.

[32] X Zhang, Z Jin, Y Li, S Li, G Lu. Photosensitized reduction of water to hydrogen using novel Maya blue-like organic–inorganic hybrid material.JColl Interface Sci, 333 (1) 2009, 285-93.

[33] A Pron, P Rannou. Processible conjugated polymers: from organic semiconductors to organic metals and superconductors. ProgPolymerSci, 27(1), 2002, 135-90.

[34]FWang, S Min, Y Han, L Feng. Visible-light-induced photocatalytic degradation of methylene blue with polyaniline-sensitized TiO_2composite photocatalysts.SuperlatticeMicrost,48 (2), 2010, 170-80.

[35] S B Kondawar, S A Acharya1, S R Dhakate. Microwave assisted hydrothermally synthesized nanostructure zinc oxide reinforced polyanilinenanocomposites. Adv Mat Lett, 2(5), 2011, 362-7.

[36]A Katoch, M Burkhart, T Hwang, S S Kim. Synthesis of polyaniline/TiO_2 hybrid nanoplates via a sol-gel chemical method.ChemEng J, 192 (1) 2012, 262-8.

[37] A Pron, F Genoud, C Menardo, M Nechtschein. The effect of the oxidation conditions on the chemical polymerization of polyaniline. Synthetic Met, 24(3), 1988, 193-201.

[38] H Okamoto, M Okamoto, T Kotaka. Structure development in polyaniline films during electrochemical polymerization. II: Structure and properties of polyaniline films prepared via electrochemical polymerization. Polymer, 39(18) 1998, 4359-67.

[39] K He, M Li, L Guo. Preparation and photocatalytic activity of PANI-CdS composites for hydrogen evolution.Int J Hydrogen Energy, 37(1),2012, 755-9.

[40] T Tayeh, AS Awad, M Nakhl, M Zakhour, J-F Silvain, J-L Bobet. Production of hydrogen from magnesium hydrides hydrolysis.Int J Hydrogen Energy,39(7), 2014, 3109-17.

[41]AKoca, M Şahin. Photocatalytic hydrogen production by direct sun light from sulfide/sulfite solution. IntJHydrogen Energy, 27(4), 2002, 363-7.

[42] G Murugadoss. Synthesis and Characterization of Transition Metals Doped ZnONanorods. J Mater SciTechnol,28(7), 2012, 587-593.

[43] RJ Wen, X Fan, Z Yang, Z Tan, B Yang. Electrochemical performances of ZnO with different morphology as anodic materials for Ni/Zn secondary batteries.ElectrochimActa,83, 2012, 376-82.

[44] O Yalçın. Nanorods, JanezaTrdine 9, 51000 Rijeka, Croatia: Published by InTech, 2012.

[45] I Fechete, OErsen, FGarin, LLazar, ARach. Catalytic behavior of MnMCM-48 and WMnMCM-48 ordered mesoporous catalysts in a reductive environment: A study of the conversion of methylcyclopentane. CatalSciTechnol,3, 2013, 444-53.

[46] **S** Haddoum, IFechete, BDonnio, FGarin,DLutic, CEChitour.Fe-TUD-1 for the preferential rupture of the substituted CC bond of methylcyclopentane (MCP).CatalComm,27, 2013, 141-7.

[47]BPall**,** MSharon. "Enhanced photocatalytic activity of highly porous ZnO thin films prepared by sol–gel process". MaterChemPhys,76, 2002**,** 82-7.

[48] S Suwanboon, P Amornpitoksuk, AHaidoux, JC Tedenac. Structural and optical properties of undoped and aluminium doped zinc oxide nanoparticles via precipitation method at low temperature. J AllysCompd,462, 2008, 335-9.

[49] H Yang, S Nie. Preparation and characterization of Co-doped ZnOnanomaterials.Mater ChemPhys,114, 2009, 279-82.

[50] IK El Zawawi, RA AbdAlla. Electrical and optical phototransformation properties in As doped Se thin films. Thin solid films,339 (1-2), 1999, 314-9.

[51] L Zhang, P Liu, Z Su. Preparation of PANI-TiO_2nanocomposites and their solid-phase photocatalytic degradation.PolymDegradStabil,91, 2006, 2213-9.

[52]C Luo, D Li, W Wu, Y Zhang, C Pan. Preparation of porous micro–nano-structure NiO/ZnOheterojunction and its photocatalyticproperty.RSC Adv,4, 2014, 3090-5.

[53] T Lyubina, D V Markovskaya, E A Kozlova, VN Parmon. Photocatalytic hydrogen evolution from aqueous solutions of glycerol under visible light irradiation.Int J Hydrogen Energy,38, 2013, 14172-9.

[54] X Zhang, D Jing, LGuo. Effects of anions on the photocatalytic H_2 production performance of hydrothermally synthesized Ni-doped $Cd_{0.1}Zn_{0.9}S$ photocatalysts. Int J Hydrogen Energy,35, 2010, 7051-7.

[55] AA Nada, MH Barakat, HA Hamed, NR Mohamed, TN Veziroglu.Studies on the photo catalytic hydrogen production using suspended modified TiO_2photocatalysts.Int J Hydrogen Energy,30, 2005, 687-91.

[56] B Zielinska, EB Palen, RJ Kalenczuk. Photocatalytic hydrogen generation over alkaline-earth titanates in the presence of electron donors.Int J Hydrogen Energy,33, 2008, 1797-802.

[57] Y Li, F He, S Peng, G Lu, S Li.Photocatalytic H_2 evolution from NaCl saltwater over $ZnS_{1-x-0.5y}O_x(OH)_y$–ZnO under visible light irradiation. Int JHydrogenEnergy, 36(17),2011, 10565-73.

[58]J Wang, Z Wang, B Huang, Y Ma, Y Liu, X Qin, X Zhang, Y Dai. Oxygen Vacancy Induced Band-Gap Narrowing and Enhanced Visible Light Photocatalytic Activity of ZnO. ACS Appl Mater Interfaces, 4(8),2012, 4024-30.

[59]SC Das, RJ Green, J Podder, TZ Regier, GS Chang, A Moewes.Band Gap Tuning in ZnOThrough Ni Doping via Spray Pyrolysis. J PhysChem C,117(24), 2013, 12745-53.